Catal Lett (2009) 129:215–221
DOI 10.1007/s10562-008-9792-y

The Support Effect over Pt–$H_3PW_{12}O_{40}$ Based Metal-Acid Bifunctional Catalysts on the Catalytic Performance in *n*-Pentane Isomerization

Yuandong Xu · Xia Zhang · Hongling Li · Yanxing Qi · Gongxuan Lu · Shuben Li

Received: 11 November 2008 / Accepted: 18 November 2008 / Published online: 4 December 2008

Abstract The effects of the support materials (γ-Al_2O_3, SiO_2, ZrO_2) on the catalytic performance in *n*-pentane isomerization have been investigated for Pt–$H_3PW_{12}O_{40}$ (Pt–TPA) metal-acid bifunctional catalysts. Significant impact of supports on the catalyst activity has been found and the activity sequence corresponding to different supports was ZrO_2 >>SiO_2 >>γ-Al_2O_3. Several characterization methods of XRD, FT-IR, NH_3-TPD, TPR and BET were used to explore the nature of the supported catalysts. Simultaneously, the influence of a series of pretreatment conditions of pH, calcination temperature and calcination time for self-prepared ZrO_2 on the catalytic performance related to the supported Pt–TPA catalysts was studied.

Keywords Skeletal isomerization · Tungstophosphoric acid · Support effect · ZrO_2 · SiO_2 · γ-Al_2O_3

Y. Xu · X. Zhang · H. Li · Y. Qi (✉) · G. Lu (✉) · S. Li (✉)
State Key Laboratory for Oxo Synthesis and Selective Oxidation, Lanzhou Institute of Chemical Physics, Chinese Academy of Sciences, Lanzhou 730000, People's Republic of China
e-mail: qiyx@lzb.ac.cn

G. Lu
e-mail: gxlu@lzb.ac.cn

S. Li
e-mail: lisb@lzb.ac.cn

Y. Xu · X. Zhang · H. Li
The Graduate University of the Chinese Academy of Sciences, Beijing 100049, People's Republic of China

1 Introduction

The skeletal isomerization of *n*-alkanes plays an important role in the production of high-octane number isoparaffins as an effective octane number enhancer for the gasoline pool due to the more and more stringent environmental legislations regarding the gradually improved gasoline quality. In general, chlorinated Pt/Al_2O_3 or Pt/mordenite has been traditionally used as catalyst for the above commercial approach. Because of some disadvantages known to us for these commercial catalysts in their practical application process, in recent years much attention has been paid to the solid acid materials, such as sulfated zirconia [1, 2] and tungstated zirconia [3, 4], and heteropoly compounds [5, 6].

In particular, heteropoly anions based on the Keggins structure have been utilized in many heterogeneous and homogeneous catalytic reactions [7, 8], among which TPA has been extensively studied in lots of acid catalyzed reactions because of its very strong acidity. However, TPA has a very low surface area (<10 m^2/g), which hinders its practical utilization as a solid acid. Considering that, supporting TPA on solids with high surface area may be a useful method for improving catalytic performance. In this way, many studies have been done lately using a great variety of supports: carbons [9, 10], silica [11], aluminas [12, 13], etc. Bifunctional catalysts consisting of Pt and heteropoly compounds were reported to be highly active and selective for skeletal isomerization of alkanes. Liu et al. [14] found that the steady state activity and selectivity of $Cs_{2.5}H_{0.5}PW_{12}O_{40}$ in *n*-C_4 and *n*-C_5 isomerization, were greatly enhanced by the addition of Pt or Pd in the presence of hydrogen. Moreover the benefit of Pt addition was also observed in the absence of hydrogen. Recently, we evaluated the catalytic performance of MCM-41 [15]

and zirconia [16] supported Pt–TPA catalysts in hydroisomerization of *n*-pentane and observed high catalytic activity and *iso*-pentane selectivity.

Many researchers have shown that the behavior of the catalysts is strongly affected by the support material and most studies of supported noble metal-heteropoly acids catalysts for *n*-alkanes isomerization have been made using different support materials. Therefore, it is of interest to study how different support materials influence the catalytic performance of the catalysts. This study focused on Pt–TPA based bifunctional catalysts and the influence of support materials. Three different support materials were chosen for the investigation, i.e. γ-Al_2O_3, SiO_2, and ZrO_2. Their effect on the catalyst performance has been addressed. In addition, in our experimental conditions ZrO_2 supported Pt–TPA catalyst exhibited the most effective isomerization activity, the influence of pretreatment conditions of pH, calcination temperature and calcination time for self-prepared ZrO_2 on the catalytic performance were also investigated.

2 Experimental

2.1 Catalyst Preparation

2.1.1 Supports

The supports used were γ-Al_2O_3, SiO_2 and ZrO_2. The former two supports were purchased and ZrO_2 was self-prepared referenced [17] as follows: Approximately 20 g of $ZrOCl_2 \cdot 8H_2O$ was dissolved in distilled water. Then, dilute aqueous ammonia was added drop-wise to this clear solution from a burette under vigorous stirring until the pH of the solution reached the requirement value. The obtained $Zr(OH)_4$ precipitate was washed with distilled water until free from chloride ions and dried at 110 °C for 24 h, and calcined under air atmosphere to produce ZrO_2.

2.1.2 Supported Pt–TPA

Samples of Pt–TPA supported on γ-Al_2O_3, SiO_2 and ZrO_2 were prepared by conventional impregnation methods using hexachloroplatinic acid and TPA as the precursors. After impregnation for 70 min at room temperature, the solvent was evaporated and the solids obtained were dried at 110 °C overnight and calcined at 300 °C for 5 h. The Pt and TPA loadings were constant of 1% and 30% according to our previously reported paper [16].

2.2 Characterization

Powder XRD analysis was performed to verify the species in the catalysts. XRD patterns of the samples were recorded on a Rigaku D/MAX-RB X-ray diffractometer with a Cu Kα target operated at 50 kV and 40 mA with a scanning speed of 0.5°/min. FT-IR spectroscopy was carried out on a Bruker IFS 120 FT-IR spectrometer using ca. 0.5 mm KBr pellets containing 2.5 mass% sample. The acid properties of the samples were measured by NH_3-TPD experiments. Each catalyst (0.1 g) was charged into a tubular quartz reactor of the conventional TPD apparatus. The catalyst was pretreated at 300 °C for 1.5 h under a flow of N_2 (20 mL/min) to remove any physisorbed organic molecules. Twenty milliliters of NH_3 was then pulsed into the reactor every minute at 100 °C until the acid sites were saturated with NH_3. The physisorbed NH_3 was removed by evacuating the catalyst sample at the same temperature for 2 h. The furnace temperature was increased from 100 °C to 800 °C. The desorbed NH_3 was detected using a TCD detector. H_2-TPR of the catalyst was performed at atmospheric pressure in a conventional flow system built in our laboratory at a linearly programmed rate of 10 °C/min from 20 °C to 800 °C (5% H_2 in a Ar stream with a flow rate of 40 mL/min). Sample of 50 mg was used for each run. The amount of the consumed H_2 was determined by a thermo-conductivity detector (TCD). Before each measurement, the samples were purged with dry air at 400 °C for 1 h. The specific surface areas of the supports were determined by BET method on a Micromeritics ASAP 2010 apparatus at a liquid nitrogen temperature with N_2 as the absorbent at −196 °C.

2.3 Catalytic Performance Evaluation

The catalytic reaction of *n*-pentane isomerization was carried out in a fixed-bed quartz microtube reactor (8 mm i.d.) under atmospheric pressure. A 0.5 g portion of the catalyst was loaded into the reactor and activated in situ at 200 °C for 90 min in H_2 flow (30 mL/min). The reactant mixture of *n*-pentane, hydrogen and nitrogen was fed through the catalyst bed and reacted at 200 °C with the flow rates of 0.62, 2 and 10 mL/min, respectively. The reaction products were analyzed using an on-line GC 7890 gas chromatograph equipped with a capillary column (plot Al_2O_3/KCl, 30 m × 0.32 mm) connected to a flame ionization detector. The overall conversions were calculated using correction factors corresponding to reactant and products.

3 Results and Discussion

3.1 Characterization of the Samples

Figure 1 shows the powder XRD of γ-Al_2O_3, SiO_2, ZrO_2 and 1% Pt–30%TPA loadings supported on them. γ-Al_2O_3

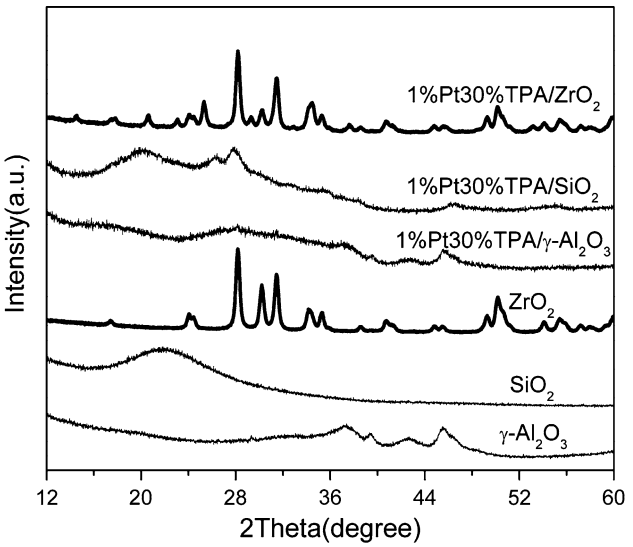

Fig. 1 XRD patterns of ZrO_2, SiO_2, γ-Al_2O_3 and their supported catalysts

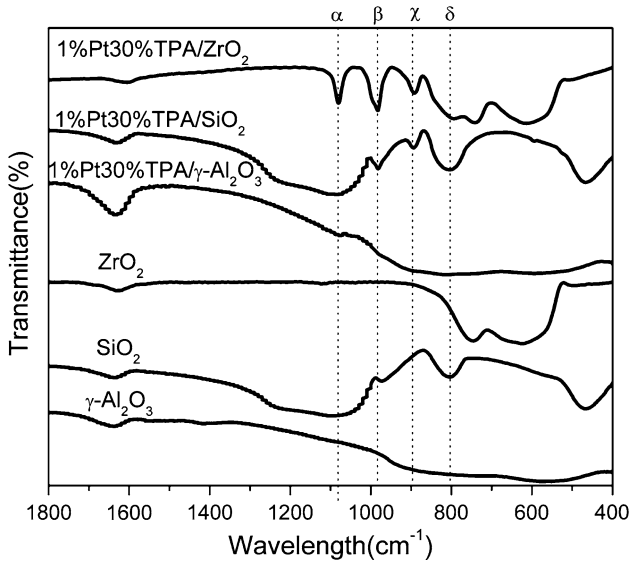

Fig. 2 FT-IR spectra of samples for ZrO_2, SiO_2, γ-Al_2O_3 and their supported catalysts

showed two characteristic diffraction peaks centered at 37.5° and 45.9° [18]. A wide diffraction structure peaked at 22° for SiO_2, which is typical of amorphous nature of the material, was observed, There are two crystal phase corresponding to ZrO_2, which are located at 28.1° and 31.4° for the monoclinic phase and at 30.1 for the tetragonal phase [16]. When Pt and TPA were loaded new diffraction peaks, which could be attributed to TPA, emerged on the three supports except the characteristic peaks for the support themselves. For ZrO_2 supported catalyst, the intensity of the peak assigned for the tetragonal phase decreased compared to the counterpart in bulk support indicating that the crystal structure of ZrO_2 partly changed. However, after the treatment during the preparation of the supported catalyst the crystallization of amorphous SiO_2 did not occur and the crystal structure for γ-Al_2O_3 did not change. Due to the relatively low Pt content in samples, it is quite difficult to identify any diffraction corresponding to Pt species.

The supports and supported Pt–TPA species were however detected during the FT-IR absorption experiments as shown in Fig. 2. The Keggins structure of TPA on ZrO_2 was confirmed by FT-IR spectroscopy, the sample displayed four bands located between 800 and 1110 cm^{-1} which were attributed to the absorption modes of the Keggin primary structure of the $[PW_{12}O_{40}]^{3-}$ [19, 20]. These peaks at 1080 (α), 985 (β), 893 (χ) and 812 cm^{-1} (δ) correspond to the four stretching modes of the oxygen atoms bonded to tungsten and phosphorus and have been assigned to n(P–O); n(W–O) and n(W–O–W) edge and n(W–O–W) corner. From the FT-IR spectrum associated with SiO_2 supported sample only one TPA characteristic absorption peak located at 893 cm^{-1} was observed. Nearly no peaks corresponding to TPA on γ-Al_2O_3 has been found. It is known that even low concentration of TPA on the support would produce very strong characteristic absorption. However, the SiO_2 and γ-Al_2O_3 supported samples were not such case. At the same time the characteristic X-ray diffraction peaks for TPA on the two types of supports was not evident (see Fig. 1) and also from the catalyst activity comparison in Table 1 we know that the SiO_2 and γ-Al_2O_3 supported catalysts showed very low catalytic activity. According to these experiment results it is assumed that TPA may generate much stronger interaction with ZrO_2 than with other two supports.

Figure 3 shows the NH_3-TPD profiles of ZrO_2, TPA and SiO_2, γ-Al_2O_3, ZrO_2 supported 1%Pt–30%TPA catalysts. Pure ZrO_2 shows one negligible low-temperature desorption peak at about 150 °C which is attributed to NH_3 adsorbed on weak Lewis-sites. It is known that NH_3 can interact with acid sites of the bulk heteropolyacid [21]. A sharp peak at about 600 °C was observed from NH_3-TPD of TPA, which was in good agreement with the reported value [22]. In contrast, the profiles of supported catalysts with different supports consisted of a few broad peaks. Notably, ZrO_2 supported catalyst produce a negligible weak strength and a sharp NH_3 desorption peak near

Table 1 Skeletal isomerization of *n*-pentane over Pt–TPA supported on different supports for 150 min

Support	S_{BET}(m^2/g)	Conversion (%)	Selectivity (%)			
			C_1–C_3	C_4	*i*-C_5	C_6
ZrO_2	30	65.9	0.1	1.3	97.6	1.0
SiO_2	380	20.8	–	1.1	98.4	0.5
γ-Al_2O_3	160	3.9	7.2	2.6	90.2	–

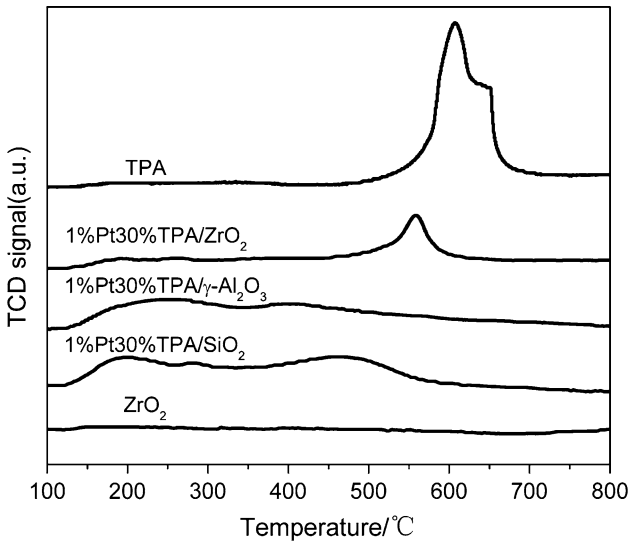

Fig. 3 NH_3-TPD profiles of selected samples

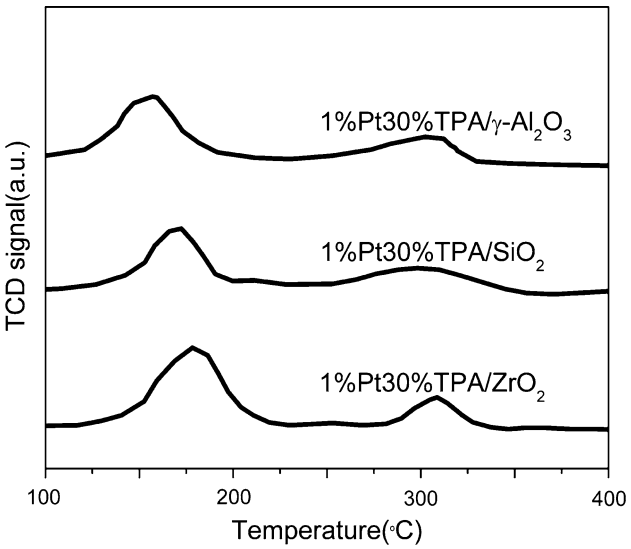

Fig. 4 Temperature programmed reduction profiles of samples with Pt

550 °C, which was not observed for the SiO_2 and γ-Al_2O_3 supported samples. It is indicative that, after SiO_2 was used as support, the acid sites in the catalyst samples are not homogeneously distributed and hence resulting a broad distribution of acid sites with weak (around 200 °C), medium (around 300 °C) and high acid strengths (around 500 °C). Whereas samples with γ-Al_2O_3 reveal the generation of broad low-temperature desorption signals (at the range of 150–300 °C) corresponding to NH_3 adsorbed on acid sites with weak strengths and a distinct medium-temperature peak at ca. 360 °C suggesting the presence of medium acid sites. Nevertheless, one can still make justifiable comment on the overall acid strengths for ZrO_2, TPA and supported samples based on the NH_3-TPD results, which appear to obey the following trend:

$$\text{TPA} \gg 1\%\ \text{Pt-30\%TPA}/\text{ZrO}_2 > 1\%\text{Pt-30\%}\ \text{TPA}/\text{SiO}_2 > 1\%\ \text{Pt-30\%}\ \text{TPA}/\gamma\text{-Al}_2\text{O}_3 > \text{ZrO}_2$$

These results indicate that the supporting TPA on all the three supports weakens the acid strength in the bulk of TPA. Based on microcalorimetry measurements of the heat of adsorption of NH_3, Kozhevnikov and coworkers [23] reported that the acid strength of TPA decreased significantly when supported on SiO_2. Other reports [24, 25] indicate that protons of TPA react with OH groups on SiO_2 to form $-OH^{2+}(H_2PW_{12}O_{40}^{-})$. Similar interaction between TPA and –OH on ZrO_2 and γ-Al_2O_3 would still reduce the acid strength in the bulk of TPA for supported form. Nevertheless the interaction strength was different dependent on the support materials.

Figure 4 demonstrates the TPR profiles for supported Pt–TPA samples. All samples present two reduction peaks. The low temperature peak corresponds to the reduction of PtO_2 species, and the temperature is associated with the reduction of different sizes of the crystallites. It is higher for Pt–TPA/ZrO_2 (around 160 °C), which indicates a more dispersed Pt on the samples. Pt reduces at a lower temperature (around 150 °C) for Pt–TPA/SiO_2 and Pt–TPA/γ-Al_2O_3, which is indicative of larger crystal sizes and a lower dispersion of the Pt crystallites. Since all the samples have the same Pt content, then there is a part of this Pt that has become less reducible. This would confirm that a part of Pt is incorporated into the TPA Keggin structure becoming less reducible, while the other is deposited on the surface of the support or supported TPA. The peak at higher temperature (ca. 300 °C) probably corresponds to the joint reduction of the Pt incorporated into the TPA Keggin structure.

3.2 Effects of Different Supports on the Catalytic Performance of Pt–TPA Based Catalyst

n-Pentane conversion, products selectivity over Pt–TPA supported on different supports are shown in Table 1. Comparatively, it is very evident that ZrO_2 as support demonstrates excellent catalytic performance, though the surface area of ZrO_2 is the lowest. Generally, support with high surface area can help to disperse and distribute more active sites on itself, but in the Pt–TPA catalyst system it is clearly that the surface area is not the critical factor to influence the catalytic performance of the catalyst. When SiO_2 and γ-Al_2O_3 are used as supports, the conversion of the reactant decreased markedly. The ZrO_2 supported Pt–TPA catalyst could generate more strong acid strength (see Fig. 3) and promote the dispersion of the noble metal (see Fig. 4) in comparison with the other two supports supported samples, which may interpret the

high catalytic performance for catalyst with ZrO_2 as support. The order of the catalytic activity for catalysts corresponding to the different supports is ZrO_2 >>-SiO_2 >>γ-Al_2O_3, coinciding with the acid strength of the supported samples.

3.3 Effect of the Calcination Temperature for ZrO_2 on the Catalytic Performance

Figure 5a exhibits the effect of calcination temperature for ZrO_2 on the catalytic performance of the Pt–TPA/ZrO_2 catalysts. It can be seen that the calcination temperature of ZrO_2 has great influence on the catalytic activity. When the calcination temperature was 350 °C the corresponding catalyst exhibited the lowest reactant conversion, though the selectivity is much higher. With the increasing of the temperature the conversion increased firstly and then decreased gradually. The maximum *n*-pentane conversion appeared at 550 and 650 °C. However the selectivity of the *iso*-pentane for the later was higher than that related to the former. As a result the optimum ZrO_2 calcination temperature should be at 650 °C.

The effect of calcination temperature on the ZrO_2 crystal phase was demonstrated in Fig. 5b. At 350 °C, the crystal phase of ZrO_2 was mainly tetragonal (2θ = 30.1°) [16]. The monoclinic crystal phase appeared when the calcination temperature was improved to 450 °C (2θ = 28.4 and 31.4°) [16]. The monoclinic phase gradually increased before 650 °C and maintained that intensity even at higher temperature. On the contrary, the tetragonal phase remained nearly the same before 650 °C and rapidly decreased as soon as the calcination temperature was further improved. If we correlated the catalyst activity with the ZrO_2 crystal phase, it can be observed that when the diffraction peak intensities for the tetragonal and monoclinic phases were both high, i.e. the ZrO_2 was calcined at 650 °C, the supported Pt–TPA catalyst exhibited the highest catalytic activity.

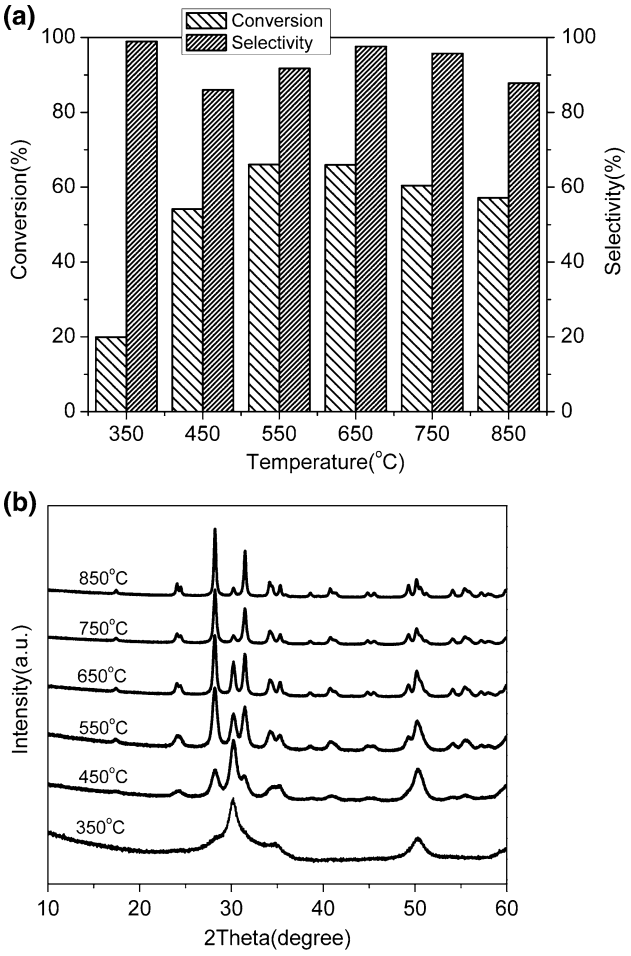

Fig. 5 **a** Effect of ZrO_2 calcination temperature on the catalytic performance of Pt–TPA/ZrO_2 and **b** Crystal phase transformation for ZrO_2 along with the calcination temperature

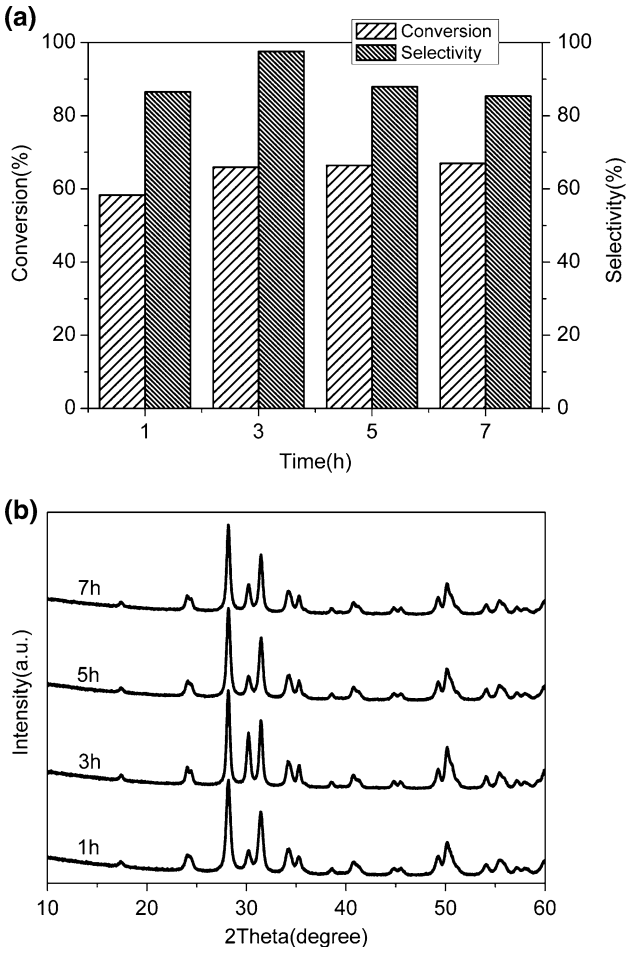

Fig. 6 **a** Effect of ZrO_2 calcination time at 650 °C on the catalytic performance of Pt–TPA/ZrO_2 and **b** Crystal phase transformation for ZrO_2 along with the calcination time

3.4 Effect of the Calcination Time for ZrO_2 on the Catalytic Performance

Our results clearly demonstrate that the catalytic performances of Pt–TPA/ZrO_2 catalysts are dependent on the ZrO_2 calcination time. From Fig. 6a it can be seen that both of the catalytic conversion and selectivity of skeletal isomerization were the lowest with the 1 h calcination time. Prolonging the calcination time to 3 h the activity of Pt–TPA/ZrO_2 reached the highest with 65.9% conversion and 97.6% selectivity. Further increasing the ZrO_2 calcination time attained to 5 and 7 h the conversion of the reactant remained nearly the same to that corresponding to 3 h and the selectivity of *iso*-pentane decreased remarkedly. In our experiments, 3 h is the optimal ZrO_2 calcination time, but it is highly likely that such value could be relevant to the calcination temperature (see Fig. 5a, b). At the same time, analysis from Fig. 6a and b it can be concluded that the low percentage of tetragonal phase in ZrO_2 corresponds to the low activity of the related supported catalyst, which was in accordance with the analysis result in the above section.

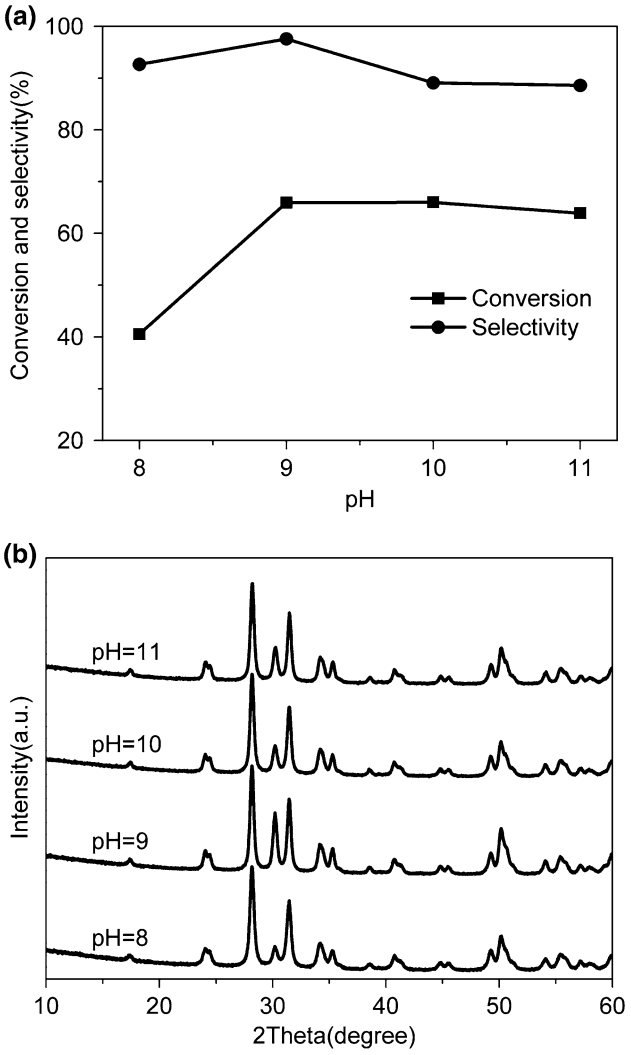

Fig. 7 **a** Effect of pH for preparation of ZrO_2 on the catalytic performance of Pt–TPA/ZrO_2 and **b** Crystal phase transformation for ZrO_2 along with the pH values

3.5 Effect of pH for ZrO_2 on the Catalytic Performance

Figure 7a shows the catalytic performance of zirconia supported Pt–TPA catalysts in the *n*-pentane isomerization at 200 °C after a 150 min reaction, plotted as a function of pH value. Conversion of *n*-pentane and selectivity for *iso*-pentane were very high at pH value of 9, but drastically for selectivity and slightly for conversion decreased with increasing pH value (pH > 9). When ZrO_2 was prepared at low pH value of 8, the reactant conversion was as low as 40%. Among the catalysts tested, the zirconia supported Pt–TPA catalyst, in which the zirconia was prepared at pH = 9, showed the best catalytic performance. The XRD patterns for ZrO_2 with different pH values are shown in Fig. 7b. The transformation trend of the crystal phase was nearly the same to Fig. 6b, i.e. the highest activity of the supported catalyst the highest percentage of tetragonal phase in the corresponding zirconia support. From the experiment results, it is suggested that the percentage of the tetragonal phase in the zirconia support should be responsible for the change of the catalytic activity.

4 Conclusions

The catalytic activity of the supported Pt–TPA catalysts with different supports for *n*-pentane skeletal isomerization to *iso*-pentane is in the order: ZrO_2 >>SiO_2 >>γ-Al_2O_3. ZrO_2 as support exhibits much better catalytic performance than other high surface area supports, indicating that in Pt–TPA based catalyst system the surface area for supports is not a critical factor to influence the catalytic activity. The synergistic effects of the strong acid sites and the highly dispersion noble metal sites offered by Pt–TPA significantly improve the catalytic activity of the ZrO_2 supported catalyst. The correlation of the catalyst performance with the support crystal phase suggested that ZrO_2 with both strong tetragonal and monoclinic crystal phase is advantageous to the catalyst activity. 650 °C is the optimal ZrO_2 calcination temperature in our experimental conditions. The calcination time and the pH for preparing ZrO_2 at 3 h and 9, respectively, should be suitable. Low values of the calcination time (<3 h) and pH (<9) generated low reaction conversion, but too high values of those would decrease the *iso*-pentane selectivity.

References

1. Li XB, Nagaoka K, Olindo R, Lercher JA (2006) J Catal 238:39
2. Kim SY, Lohitharn N, Goodwin JG Jr, Olindo R, Pinna F, Canton P (2006) Catal Commun 7:209
3. Hernandez ML, Montoya JA, Hernandez I, Viniegra M, Llanos ME, Garibay V, Del Angel P (2006) Micropor Mesopor Mater 89:186
4. Vu TN, Van Gestel J, Gilsona JP, Collet C, Dath JP, Duchet JC (2005) J Catal 231:453
5. Miyaji A, Echizen T, Nagata K, Yoshinaga Y, Okuhara T (2003) J Mol Catal A Chem 201:145
6. Liu YY, Na K, Misono M (1999) J Mol Catal A Chem 141:145
7. Guo YH, Hang CG (2007) J Mol Catal A Chem 262:136
8. Kumbar SM, Halligudi SB (2007) Catal Commun 8:800
9. Izmi Y, Urabe K (1981) Chem Lett 27:663
10. Chu W, Yang X, Ye X, Wu Y (1996) Langmuir 12:4185
11. Kasztelan S, Payen E, Moffat JB (1990) J Catal 125:45
12. Ehwald H, Fiebig W, Jerschkwitz HG, Lischke G, Parlitz B, Reich P, Ohlmann G (1987) Appl Catal 34:32
13. Rao KM, Gobetto R, Iannibello A, Zecchina A (1989) J Catal 119:512
14. Liu Y, Koyano G, Misono M (2000) Top Catal 11:239
15. Xu YD, Qi YX, Lu GX, Li SB (2008) Catal Lett 125:83
16. Xu YD, Zhang X, Li HL, Qi YX, Lu GX, Li SB (2008) Catal Lett 125:340
17. Zhai YF, Zhang HM, Hua JW, Yi BL (2006) J Membr Sci 280:148
18. Wang F, Xu XL, Sun KP (2008) React Kinet Catal Lett 93:135
19. Misono M (1987) Catal Rev Sci Eng 29:269
20. Edwards JC, Thiel CY, Bernac B, Knifton JF (1998) Catal Lett 51:77
21. Okuhara T, Mizuno N, Misono M (1996) Adv Catal 41:113
22. Lee SH, Park DR, Kim H, Lee J, Jung JC, Woo SY, Song WS, Kwon MS, Song IK (2008) Catal Commun 9:1920
23. Kapustin GI, Brueva TR, Klyachko AL, Timofeeva MN, Kulikov SM, Kozhevnikov IV (1990) Kinet Catal 31:896
24. Mastihkin VM, Kulikov SM, Nosov AV, Kozhevnikov IV, Mudrakovsky IL, Timofeeva MV (1990) J Mol Catal 60:65
25. Lefebvre F (1992) J Chem Soc Chem Commun 756